OUKA
The University of Osaka
Institutional Knowledge Archive

Title	Structural basis of effector recognition by the T3SS chaperone VecA from Vibrio parahaemolyticus
Author(s)	Iimori, Minato; Oki, Hiroya; Akeda, Yukihiro et al.
Citation	Biochemical and Biophysical Research Communications. 2025, 776, p. 152190
Version Type	VoR
URL	https://hdl.handle.net/11094/102613
rights	This article is licensed under a Creative Commons Attribution 4.0 International License.
Note	

The University of Osaka Institutional Knowledge Archive : OUKA

https://ir.library.osaka-u.ac.jp/

The University of Osaka

Biochemical and Biophysical Research Communications 776 (2025) 152190

Contents lists available at ScienceDirect

Biochemical and Biophysical Research Communications

journal homepage: www.elsevier.com/locate/ybbrc

Structural basis of effector recognition by the T3SS chaperone VecA from *Vibrio parahaemolyticus*

Minato Iimori [a,1], Hiroya Oki [b,1], Yukihiro Akeda [b,c,d], Eiji Ishii [b], Toshio Kodama [f], Takumi Ueda [a], Shota Nakamura [b,e,g], Shigeaki Matsuda [b,*], Kazuki Kawahara [a,e,**], Tetsuya Iida [b,e]

[a] *Graduate School of Pharmaceutical Sciences, The University of Osaka, Suita, Osaka, 565-0871, Japan*
[b] *Research Institute for Microbial Diseases, The University of Osaka, Suita, Osaka, 565-0871, Japan*
[c] *Department of Bacteriology I, National Institute of Infectious Diseases, Japan Institute for Health Security, Shinjuku-ku, Tokyo, 162-8640, Japan*
[d] *Graduate School of Medicine, The University of Osaka, Suita, Osaka, 565-0871, Japan*
[e] *Center for Infectious Disease Education and Research, The University of Osaka, Suita, Osaka, 565-0871, Japan*
[f] *Department of Bacteriology, Institute of Tropical Medicine, Nagasaki University, Nagasaki, 852-8523, Japan*
[g] *Integrated Frontier Research for Medical Science Division, Institute for Open and Transdisciplinary Research Initiatives, The University of Osaka, Suita, Osaka, 565-0871, Japan*

ARTICLE INFO

Keywords:
Vibrio parahaemolyticus
Type III secretion system
Chaperone
Effector
Protein crystallography

ABSTRACT

Many pathogenic gram-negative bacteria utilise the type III secretion system (T3SS), a specific protein injection apparatus, to translocate virulence effectors into host cells, modulating host cell functions and establishing infection. To facilitate the precise cytosolic transport of effectors to T3SS, a class of proteins called chaperones plays a crucial role. However, a limited number of available structural data on chaperone-effector complexes hampers understanding of the mechanisms underlying this process. In *Vibrio parahaemolyticus*, a major causative agent of seafood-associated acute gastroenteritis in humans, T3SS chaperone VecA transports its cognate membrane-disrupting effector, VepA. Here, we determined the crystal structure of VecA alone and in complex with VepA at resolutions of 2.20 Å and 2.49 Å, respectively. While the overall protein fold and the hydrophobic cleft that accommodates an N-terminal β-motif of effectors were conserved among T3SS chaperones, the structural analysis revealed that surface residues are remarkably different, reflecting their substrate specificity. Additionally, unlike other reported structures of the T3SS chaperone-effector complexes, in which the effectors are partially unfolded and wrapped around the chaperone, VepA adopts a highly folded conformation in the complex. This compact structure appears to protect the fragile glycine-rich transmembrane domain of VepA and suggests that upon secretion, VepA undergoes conformational changes, including α-helix formation, allowing the transmembrane domain to embed into and disrupt the membrane of organelles containing its binding target, V-ATPase. These findings elucidate the chaperone-mediated regulation of effector transport and function of the bacterial virulence-related T3SS.

1. Introduction

Pathogenic gram-negative bacteria secrete virulence effectors to manipulate host cells, facilitate infection, and cause disease. Effectors are delivered via secretion systems, of which the type III secretion system (T3SS) is widely studied [1]. In the T3SS, newly synthesised effectors are initially recognised by chaperones and translocated to the host cell cytosol via a needle-like secretion apparatus [2]. Chaperones, which are structurally conserved in T3SS systems, are implicated in the selective recognition of the substrate, stabilisation of its structure, and maintenance of its conformation for effective secretion [3].

Vibrio parahaemolyticus, a gram-negative marine bacterium, is a major foodborne pathogen that causes acute gastroenteritis in humans [4,5]. *V. parahaemolyticus* translocates effectors into host cells using two

* Corresponding author. Research Institute for Microbial Diseases, The University of Osaka, Suita, Osaka, 565-0871, Japan.
** Corresponding author. Graduate School of Pharmaceutical Sciences, The University of Osaka, Suita, Osaka, 565-0871, Japan.
E-mail addresses: matsudas@biken.osaka-u.ac.jp (S. Matsuda), kkkazuki@phs.osaka-u.ac.jp (K. Kawahara).
[1] These authors contributed equally to this study.

https://doi.org/10.1016/j.bbrc.2025.152190
Received 27 May 2025; Accepted 9 June 2025
Available online 9 June 2025
0006-291X/© 2025 The Authors. Published by Elsevier Inc. This is an open access article under the CC BY license (http://creativecommons.org/licenses/by/4.0/).

types of T3SS: T3SS1 and T3SS2 [6,7]. Among these effectors, VepA (VP1680/VopQ), secreted via T3SS1, is a major cytotoxic factor in *V. parahaemolyticus* [8]. VepA binds to the V_0 subcomplex of V-ATPase on lysosomes and causes lysosomal membrane permeabilisation, leading to deacidification and blockage of autophagic flux [9–13]. The analysis of the cryo-electron microscopy structure of V-ATPase in complex with VepA demonstrated that in addition to the C-terminal V-ATPase-binding domain (CTD) and N-terminal chaperone-binding domain (NTD), VepA possesses a transmembrane domain (TMD) in the middle region. In the VepA–V-ATPase complex, part of the TMD of VepA is inserted into the detergent micelles surrounding V-ATPase, while the remaining part is disordered within them, implying its potential role in disrupting the lysosomal membrane [13]. The TMD of VepA is largely hydrophobic and conformationally flexible, contains multiple glycine residues (27 of 158 residues), and can disrupt membranes composed of lipids with acidic head groups [11]; thus, this domain requires tightly controlled transfer mechanisms until it encounters the V-ATPase in the host cell membrane. However, the structural basis underlying these processes is unclear.

In this study, we determined the crystal structure of VepA in complex with its cognate chaperone VecA for the first time in the genus *Vibrio* [14]. In the complex, the TMD of VepA adopts a highly folded conformation, with a potentially aggregation-prone flexible hydrophobic transmembrane helical segment masked by VecA. This conformation is markedly different from that observed in the cryo-electron microscopy structure of the VepA–V-ATPase complex. Based on these structures, we discuss the mechanisms of effector recognition and stabilisation by T3SS chaperone proteins, facilitating the successful delivery of effectors to their targets.

2. Materials and methods

2.1. Protein expression and purification

Recombinant VecA and VepA were expressed in *Escherichia coli* BL21 (DE3). For VecA, cells were transformed with plasmid pGEX-6P1 encoding VecA [14] and cultured in LB medium containing 100 μg/mL ampicillin at 37 °C until OD_{660} reached 0.6. Protein expression was induced with 1.0 mM IPTG at 20 °C for 18 h. For VepA, a TEV protease recognition site was introduced upstream of the open reading frame via PCR using phosphorylated primers (5′-ATGGTGAAT ACAACGCAAAAAATC-3′ and 5′-GCCCTGAAAGTACAGATCCTCGGA TCCGATATCAGCCATGGCCTTG-3′), and the pET30a-*vepA* plasmid was used as the template [10]. The resulting plasmid was transformed into BL21(DE3), then cultured in LB medium, and induced with 0.2 mM IPTG under the same experimental conditions. Cells were harvested, lysed via sonication, and centrifuged to remove cellular debris. GST-VecA was purified using GSTrap HP and HiTrap Q HP columns and cleaved with a Turbo3C protease. Following tag and protease removal, the protein was purified by size-exclusion chromatography (SEC) using a HiLoad 16/600 Superdex 200 pg column in 20 mM Tris-HCl, 150 mM NaCl, 2 mM DTT (pH 8.0), and concentrated to 10 mg/mL. VepA was purified using a HisTrap FF column and digested with TEV protease. The cleaved sample was reapplied to the column, and the flowthrough was further purified by SEC in a buffer containing 20 mM Tris-HCl and 150 mM NaCl (pH 8.0), yielding 10 mg/mL protein for crystallisation experiments. For complex formation, VepA and VecA were mixed at a 1:2.5 M ratio and separated from unbound proteins by SEC using a HiLoad 16/600 Superdex 200 pg column equilibrated with the same buffer supplemented with 2 mM DTT. The samples were concentrated to 8 mg/mL for crystallisation experiments.

2.2. Crystallisation, data collection, and structural analyses

Crystallisation assays were conducted at 4 °C using the sitting-drop vapour diffusion method. VecA crystals were obtained in 0.1 M Tris-HCl (pH 8.8) and 1.8 M ammonium sulfate. For phasing, crystals were soaked in 0.2 mM Ta_6Br_{12}. The VepA–VecA complex was crystallised in 100 mM sodium cacodylate (pH 6.5), 20 % (v/v) PEG 400, and 200 mM Li_2SO_4. For X-ray diffraction data collection, crystals were cryoprotected by increasing PEG 400 to 40 % before flash-freezing in liquid nitrogen. All diffraction data were collected at the beamline BL38B1 of SPring-8. The VecA crystal belonged to space group $P4_12_12$ with cell dimensions of $a = b = 73.75$ Å, $c = 109.91$ Å. Data were collected at 1.25380 Å for anomalous phasing. VepA–VecA complex crystals belonged to space group $C222_1$ with cell dimensions of $a = 109.85$ Å, $b = 152.93$ Å, $c = 101.12$ Å. For VecA crystals, phasing was performed using AutoSol from the Phenix suite [15], followed by manual model building in Coot [16] and refinement using phenix.refine [15]. The final model was refined to a resolution of 2.20 Å with R_{work} and R_{free} values of 0.239 and 0.295, respectively. For VepA–VecA complex crystals, molecular replacement was applied to determine the initial phase using Phaser from the Phenix suite [15] and the VecA structure as the search model. The VepA portion was built in Coot, and the structure was refined to a resolution of 2.49 Å with R_{work} and R_{free} values of 0.241 and 0.276, respectively. Data collection and refinement statistics are summarised in Table 1. Model validation with MolProbity [17] indicated good stereochemistry and overall quality for both structures (Table 1).

Table 1
X-ray data collection and structure refinement statistics.

Data collection	VecA (Ta_6Br_{12} derivative)	VepA-VecA
Beamline	SPring-8 BL38B1	SPring-8 BL38B1
Detector	Pilatus3 6 M	MX225HE
Wavelength (Å)	1.25380	1.00000
Space group	$P4_12_12$	$C222_1$
Unit-cell parameters (Å, °)	$a = b = 73.75$, $c = 109.91$, $\alpha = \beta = \gamma = 90.00$	$a = 109.85$, $b = 152.93$, $c = 101.12$, $\alpha = \beta = \gamma = 90.00$
Total measured reflections	382229 (33342)	195356 (24194)
Unique reflections	16059 (1354)	29792 (3334)
Resolution (Å)	47.12–2.20 (2.27–2.20)	48.26–2.49 (2.59–2.49)
R_{merge}	0.120 (1.612)	0.147 (1.108)
$CC_{1/2}$	0.999 (0.794)	0.995 (0.608)
Completeness (%)	100.0 (100.0)	99.0 (99.1)
Wilson *B*-factors ($Å^2$)	56.3	53.1
Average I/σ (I)	20.9 (2.1)	15.0 (2.0)
Redundancy	23.8 (24.6)	6.6 (7.3)
Refinement		
Resolution (Å)	32.81–2.20 (2.26–2.20)	48.26–2.49 (2.53–2.49)
Reflections	15999 (1292)	29612 (1398)
No. Atoms		
Protein	264	668
Water	18	–
Others		
Ta_6Br_{12}	1	–
PO_4	1	–
R_{work}	0.239 (0.304)	0.241 (0.348)
R_{free}	0.295 (0.346)	0.276 (0.380)
R.M.S.D. from ideal		
Bonds (Å)	0.009	0.003
Angles (°)	1.070	0.677
B-factors ($Å^2$)	68.0	68.5
Ramachandran plot analysis (%)		
Most favored	96.9	95.4
Allowed	3.1	4.3

3. Results and discussion

3.1. Structure of VecA

To elucidate the mechanism of effector recognition by the T3SS chaperone VecA from *V. parahaemolyticus*, we performed an X-ray crystallographic study on the VepA–VecA complex. Although we successfully obtained its crystals, our attempts to resolve its structure via molecular replacement utilising previously known or AlphaFold-

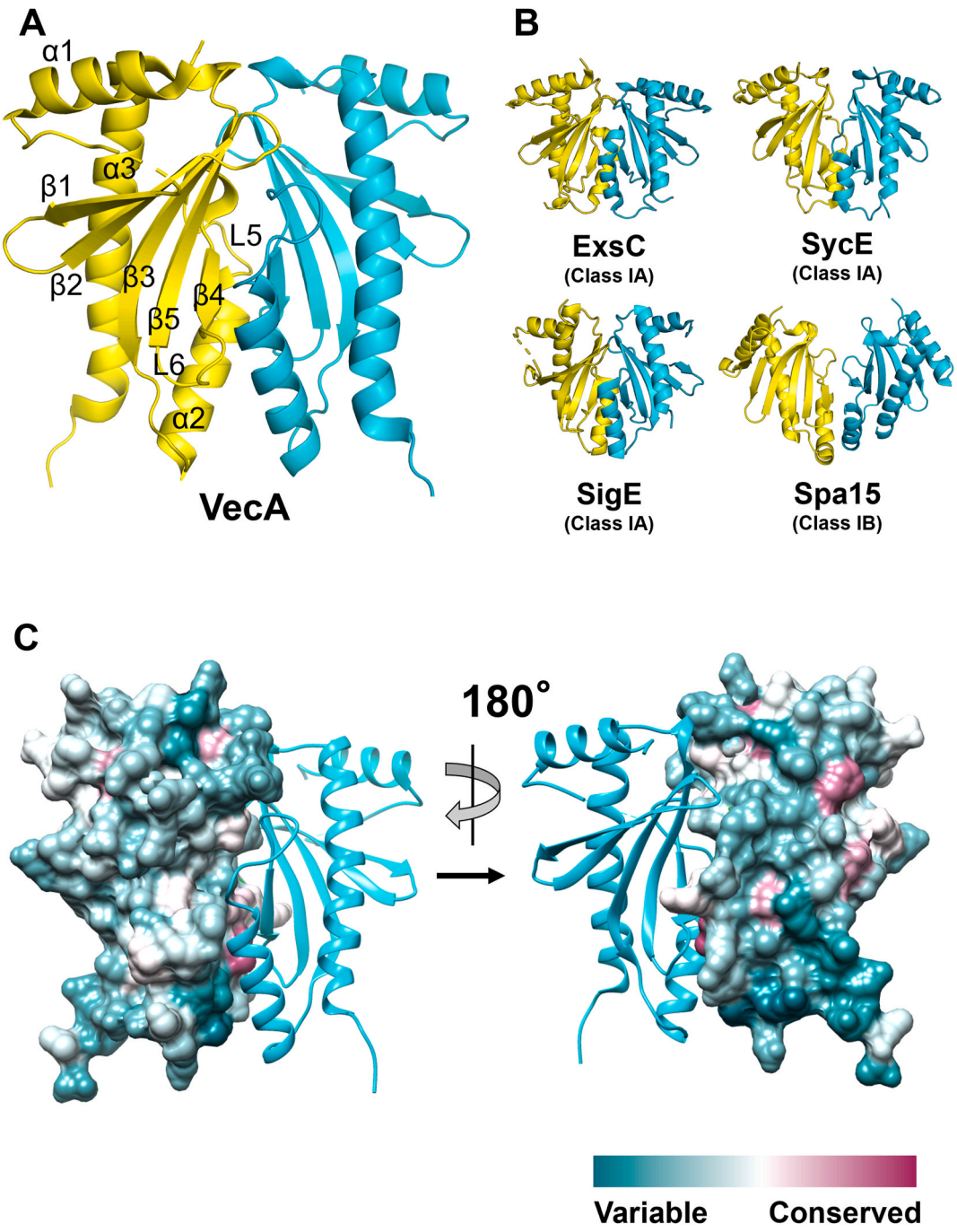

Fig. 1. Structures of the T3SS chaperone VecA. (A) Cartoon representation of the structure of the VecA dimer consisting of three α helices and five β antiparallel strands. The monomers are shown in yellow and cyan. (B) Cartoon representation of the ExsC, SycE, SigE, and Spa15 chaperones (PDB accession codes 3KXY, 1JYA, 1K3S, and 1RY9, respectively). (C) Sequence alignment and conservation of surface-exposed amino acids in class IA and IB T3SS chaperones. Multiple sequence alignments were performed using ClustalW [31], and conservation scores ranging from 0.05 (variable) to 0.7 (conserved) were calculated using UCSF Chimera [32]. The alignments are shown in Fig. S2. Amino acid conservation is depicted in a colour gradient from turquoise (highly variable) to purple (highly conserved). (For interpretation of the references to colour in this figure legend, the reader is referred to the Web version of this article.)

predicted structures were unsuccessful. Therefore, we tried to determine the structures of VepA and VecA in the free state and use them for initial phasing. Several crystallisation trials utilising various constructs of VepA resulted in precipitation in crystallisation drops, possibly due to the flexible nature of the NTD and TMD (vide infra). In contrast, we obtained crystals of VecA, and the structure was then determined at a resolution of 2.20 Å by the single anomalous dispersion method using a Ta_6Br_{12} metal ion cluster as an anomalous scatterer (Fig. 1A, Table 1). This structure represents the first reported structure of a T3SS chaperone from the genus *Vibrio*.

Similar to other T3SS chaperones, VecA forms a dimer in an asymmetric unit (Fig. 1A). Both monomers possess almost identical structures with a backbone Cα root-mean-square deviation (RMSD) value of ~0.3 Å. Each VecA monomer adopts an α1-β1-β2-β3-α2-β4-α3 fold topology, which is conserved among T3SS chaperones (Fig. S1A) [18]. The dimerisation interface is formed predominantly by α2, β4, and two loops (L5 and L6), and Y76 in L5 penetrates the hydrophobic pocket created by β4 and L6 of the adjacent monomer (Fig. S1B and C).

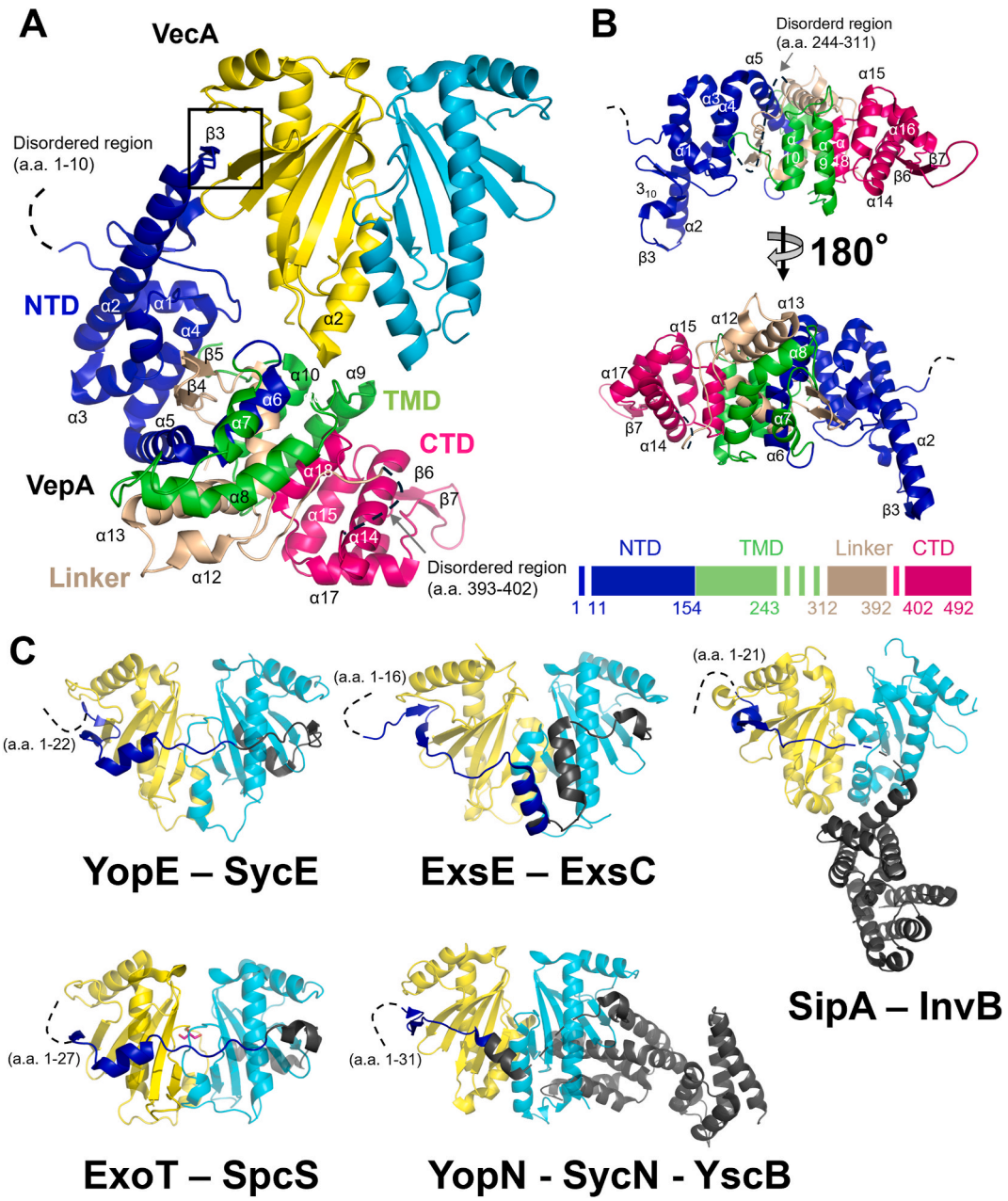

Fig. 2. Structure of chaperone-effector complexes. (A) Cartoon representation of the VepA–VecA complex. The region highlighted in Fig. 3A is indicated by a black square. (B) Structure and domains of VepA in the complex. The NTD, TMD, linker, and CTD are shown in blue, green, brown, and pink. (C) Cartoon representations of the T3SS chaperone-effector complexes YopE-SycE, ExsE-ExsC, SipA-InvB, ExoT-SpcS, and YopN-SycN-YscB (PDB accession codes 1L2W, 3KXY, 2FM8, 4JMF, and 1XKP, respectively). The N-terminal regions of effectors (residues 1–50) are highlighted in blue, and the remaining residues are shown in grey. CTD, C-terminal domain; NTD, N-terminal domain; TMD, transmembrane domain. (For interpretation of the references to colour in this figure legend, the reader is referred to the Web version of this article.)

T3SS chaperones are classified into three categories (I, II, and III) based on the type of substrate they bind to [3,19]. Class I chaperones bind to T3SS effectors and are further divided into two subclasses: class IA (a single substrate) or class IB (multiple substrates) [3,19]. Our previous study identified VecA as a class IA chaperone that specifically recognises VepA [14]. VecA shares overall protein fold with class IA T3SS chaperones—ExsC of *Pseudomonas aeruginosa*, SycE of *Yersinia pseudotuberculosis*, and SigE of *Salmonella enterica*—and class IB chaperones, including Spa15 of *Shigella flexneri* (Fig. 1B) [20–23]. Comparative sequence analyses of 16 class IA and IB chaperones revealed that despite their similar overall structures, surface regions exhibited lower sequence conservation, which might influence the specificity of chaperones to effectors (Fig. 1C–S2, and S3).

3.2. Structure of the VepA–VecA complex

The structure of VecA was utilised for molecular replacement to determine the VepA–VecA complex at a resolution of 2.49 Å (Fig. 2A). The VecA structure remained essentially unchanged upon binding to VepA (backbone Cα RMSD was approximately 0.9 Å), with only minor structural variations in β1 and β2 of one monomer (Fig. S4). The VepA structure was resolved from the NTD to the TMD (residues 11–243), linker domain (residues 312–392), and part of the CTD (residues 402–492) (Fig. 2B–S5). A portion of the NTD (residues 1–10), a segment of the CTD (residues 393–401), and the region of the TMD adjacent to the linker domain (residues 244–311) were not resolved, reflecting the flexibility of these regions.

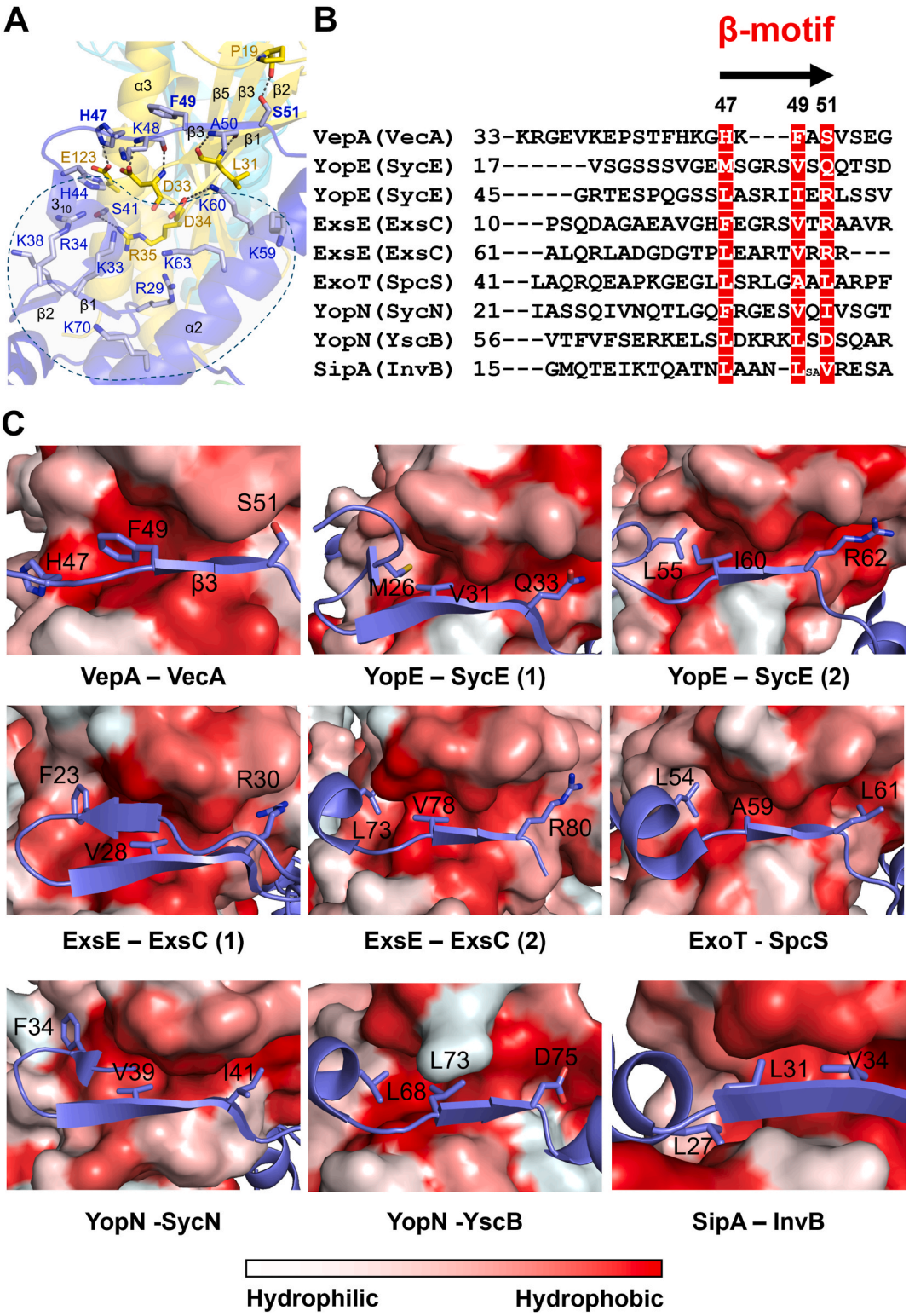

Fig. 3. Conserved regions of chaperone-effector complexes. (A) Interaction between the N-terminal domain of VepA (blue) and a VecA monomer (yellow) between β strands. Clusters of basic residues are surrounded by dashed lines. The three residues that constitute the β-motif are indicated in bold. (B) The alignment of T3SS effector sequences is shown in Fig. 2C. β-motif residues are shown in white with a red background. The β-motif residues of VepA are numbered above the alignment. (C) Detailed view of the insertion of β-strands of T3SS effectors into the hydrophobic cleft of chaperones in the complexes shown in Fig. 2C. Three key residues forming the β-motifs are shown as stick diagrams. Surface hydrophobicity gradients of chaperones are represented using the normalised consensus hydrophobicity scale [33]. In complexes with two interaction sites, both sites are shown. (For interpretation of the references to colour in this figure legend, the reader is referred to the Web version of this article.)

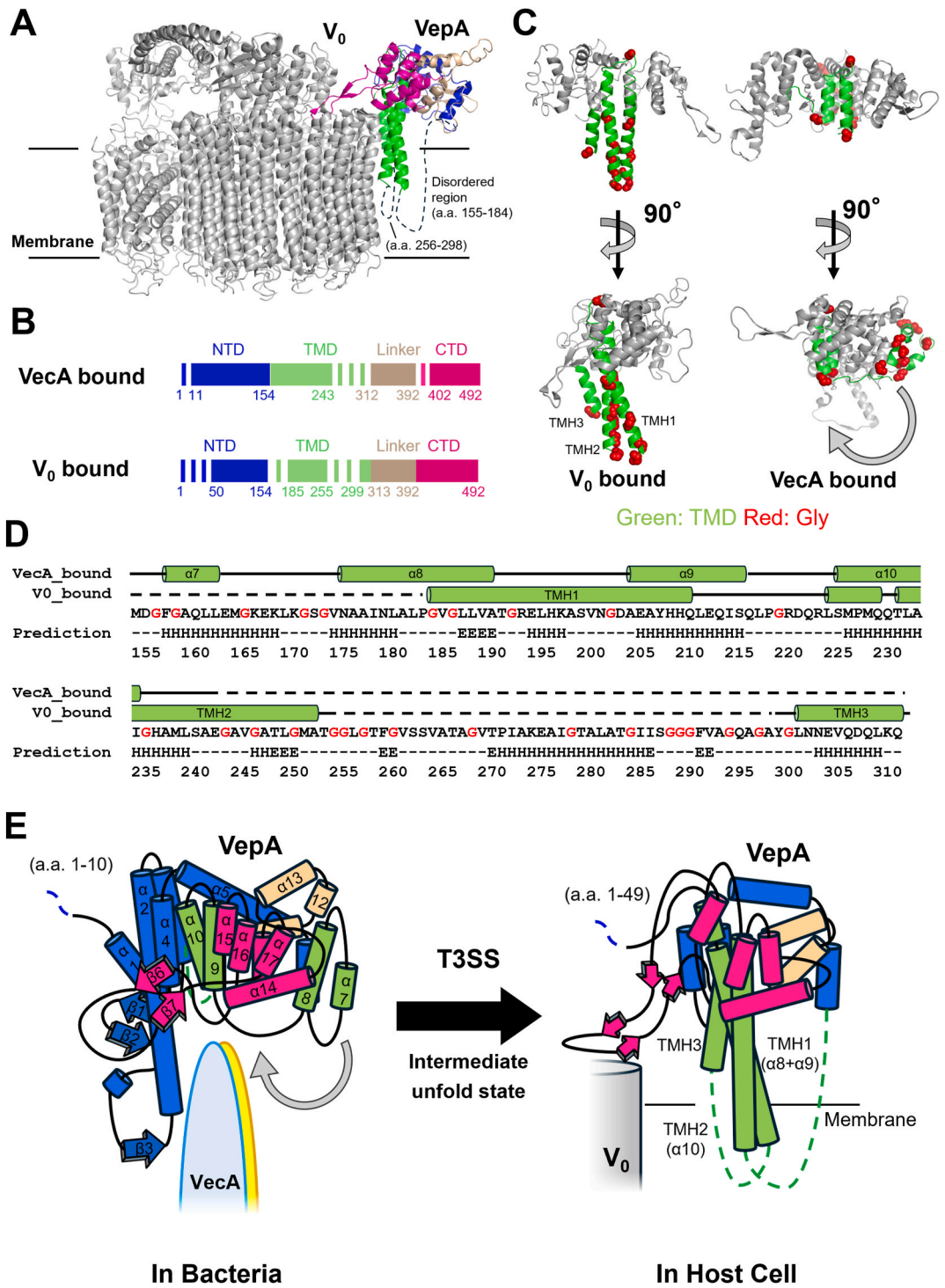

Fig. 4. Comparison of the structures of VecA-bound and V_0-bound VepA. (A) Cartoon representation of the structure of VepA bound to the V_0 subcomplex of V-ATPase (PDB accession code 6PE4). (B) Resolved residues of VepA in the VecA-bound and V_0-bound structures. (C) Structure of VecA-bound and V_0-bound VepA. The TMD is shown in green, and the other regions are shown in grey. Glycine residues are shown in red. (D) Amino acid sequence and predicted secondary structure (green) of the TMD of VecA-bound and V_0-bound VepA. Secondary structures were predicted using JPred4 [34]. Glycine residues are shown in red. (E) Structural changes in the TMD of VepA before and after secretion. CTD, C-terminal domain; NTD, N-terminal domain; TMD, transmembrane domain. Dotted lines indicate flexible disordered regions. (For interpretation of the references to colour in this figure legend, the reader is referred to the Web version of this article.)

Two VecA molecules bind to a single VepA molecule to form a 2:1 complex, similar to previously characterised T3SS chaperone-effector complexes [3]. The interaction with VecA is achieved by residues 1–154 of the NTD of VepA, consistent with our previous findings demonstrating that residues 30–100 are essential for interaction with VecA [14]. The interaction between VepA and VecA is partly similar to that of previously characterised effector-chaperone complexes (Figs. 2A, 2C, and 3) [24]. VepA β3 interacts with the edge of the β-sheet of VecA within the hydrophobic cleft (Fig. 3A). In most T3SS chaperone-effector complexes, β-motif, which comprises three key residues in the chaperone-binding β-strand and is widely conserved in T3SS substrates across animal and plant pathogens [24–26], docks into the hydrophobic

cleft [24–26] (Fig. 3B and C). In VepA, residues H47, F49, and S51 bind to the hydrophobic cleft of VecA (Fig. 3C). The amino acid composition of this β-motif varies between effectors and is not strictly limited to hydrophobic residues, suggesting that the relative contribution of this motif to binding affinity differs across complexes [24], and that variations in interaction patterns contribute to substrate selectivity. In the VepA–VecA complex, the β-strand interactions are further stabilized by amino acid residues in the 3_{10}-helix (S41), α2 (K60), and loop L4 (H47, K48) of VepA that form hydrogen bonds or salt bridges with residues in loop L1 (P19), loop L2 (D33, D34, R35), and α3 (E123) of VecA (Fig. 3A).

In contrast to the conserved β-strand-mediated interaction described above, the interaction between the remaining segment of VepA and VecA is drastically different from that found in other effector-chaperone complexes, reflecting the low sequence conservation of surface-exposed chaperone residues (Fig. 2A–C). In most complexes, the effector wraps around the chaperone, partially unfolding the NTD (Fig. 2C) [20,24,27–29]. In contrast, the NTD of VepA adopts a folded conformation and is located adjacent to VecA. While α10 in the TMD of VepA is positioned close to α2 of VecA (Fig. 2A), no direct interaction was detected. This structural feature was unexpected because NTD unfolding may be essential for secretion. However, the N-terminal 20 residues in the NTD of VepA are exposed to the solvent region, and our previous study has shown that residues 5–20 in the N-terminal region are important for secretion [14]. As the solvent-exposed flexible N-terminal region is found in other effector-chaperone complexes (Fig. 2C), the partial unfolding of the NTD may be sufficient only at the most N-terminus of effectors.

The secretory signals by which the T3SS recognises its cognate effector have not been determined. In this regard, we also identified a positively charged NTD region containing an unusually dense cluster of basic residues near a conserved hydrophobic cleft of VecA (Fig. 3A). Although this uniquely charged region of VepA may play a role in recognising the T3SS, further studies are required to confirm this hypothesis.

3.3. Conformational changes in VepA

Previous studies have demonstrated that VepA directly interacts with subunit c of the V-ATPase V_0 subcomplex in target cells and integrates its TMD into the lysosomal membrane [10,13]. The structure of the TMD of V_0-bound VepA differs substantially from that in VecA-bound VepA (Fig. 4A–C). In the V_0-bound form, over half of the TMD adopts an extended conformation, forming three transmembrane helices (TMH1-TMH3) that insert into the detergent micelles surrounding V-ATPase (Fig. 4B–D). The remaining region of TMD is disordered and thus may have a unique mode of membrane disruption (i.e., not by forming α helical pores) [13]. In the chaperone-bound state, TMH1 and TMH2 are fragmented into shorter helices (i.e., α8–α10) and are compactly folded (Fig. 4C), while the C-terminal 70 residues of the TMD, including part of TMH2 and TMH3 formed in the V_0-bound form, are disordered (Fig. 4D). The TMD contains an unusually high proportion of glycine residues (27 of 158 residues), which is unusual in membrane-embedded helices, allowing for conformational changes depending on the environment (Fig. 4B–D).

Based on these structural findings, we propose a mechanistic model for VepA secretion and function in the host cell (Fig. 4E). Initially, VepA is synthesised in a state in which its NTD and TMD exhibit flexibility, and then VecA recognises VepA and recruits it to the T3SS apparatus. At this stage, VecA interacts with VepA in a way that partially protects the fragile NTD and TMD in the bacterial cytoplasm (Fig. 4E, left panel). Upon dissociation from the chaperone, VepA is secreted through the T3SS needle complex, adopting an unfolded intermediate state [30]. Following translocation, VepA refolds and immediately binds to V-ATPase and embeds into the lysosomal membrane, culminating in membrane destabilisation (Fig. 4E, right panel) [10,13].

Effector secretion is crucial for the virulence of *V. parahaemolyticus*. As part of our effort to clarify the molecular basis of this process, we determined the structure of the class IA chaperone VecA in complex with its cognate effector VepA. Using this new information and the known structure of VepA bound to V_0 subcomplex of V-ATPase, we propose a model describing conformational changes in VepA before and after secretion. These findings elucidate the functional roles of VecA, which stabilises VepA and maintains its conformation, thereby restricting its function in bacterial cells. These results advance our understanding of tightly regulated mechanisms of chaperone-mediated effector translocation.

CRediT authorship contribution statement

Minato Iimori: Conceptualization, Data curation, Funding acquisition, Investigation, Methodology, Validation, Visualization, Writing – original draft. **Hiroya Oki:** Conceptualization, Data curation, Investigation, Methodology, Validation, Writing – original draft. **Yukihiro Akeda:** Methodology, Resources, Writing – review & editing. **Eiji Ishii:** Writing – review & editing. **Toshio Kodama:** Writing – review & editing. **Takumi Ueda:** Writing – review & editing. **Shota Nakamura:** Writing – review & editing. **Shigeaki Matsuda:** Conceptualization, Data curation, Methodology, Supervision, Validation, Writing – review & editing. **Kazuki Kawahara:** Conceptualization, Data curation, Methodology, Supervision, Validation, Writing – review & editing. **Tetsuya Iida:** Supervision, Writing – review & editing.

Data availability

Atomic coordinates and structural factors were deposited in the Protein Data Bank under accession codes 9UWZ and 9UX0 for the crystal structure of VecA and the VecA–VepA complex, respectively.

Funding

This work was supported by JSPS KAKENHI Grant Number JP24KJ1623. This work was conducted as part of "The Nippon Foundation-Osaka University Project for Infectious Disease Prevention".

Declaration of competing interest

The authors declare that they have no known competing financial interests or personal relationships that could have appeared to influence the work reported in this paper.

Acknowledgments

Synchrotron X-ray diffraction experiments were performed with the approval of the SPring-8 Proposal Review Committe (2017A2589, 2018A2553, 2019A2570, and 2024A2728).

Appendix A. Supplementary data

Supplementary data to this article can be found online at https://doi.org/10.1016/j.bbrc.2025.152190.

References

[1] W. Deng, et al., Assembly, structure, function and regulation of type III secretion systems, Nat. Rev. Microbiol. 15 (2017) 323–337, https://doi.org/10.1038/nrmicro.2017.20.
[2] Y. Akeda, J.E. Galán, Chaperone release and unfolding of substrates in type III secretion, Nature 437 (2005) 911–915, https://doi.org/10.1038/nature03992.
[3] A. Meir, et al., Substrate recruitment mechanism by gram-negative type III, IV, and VI bacterial injectisomes, Trends Microbiol. 31 (2023) 916–932, https://doi.org/10.1016/j.tim.2023.03.005.
[4] T. Honda, T. Iida, The pathogenicity of *Vibrio parahaemolyticus* and the role of the thermostable direct haemolysin and related haemolysins, Rev. Med. Microbiol. 4 (1993) 106–113, https://doi.org/10.1097/00013542-199304000-00006.

[5] S. Matsuda, et al., Advances on *Vibrio parahaemolyticus* research in the postgenomic era, Microbiol. Immunol. 64 (2020) 167–181, https://doi.org/10.1111/1348-0421.12767.
[6] K. Makino, et al., Genome sequence of *Vibrio parahaemolyticus*: a pathogenic mechanism distinct from that of *V. cholerae*, Lancet 361 (2003) 743–749, https://doi.org/10.1016/S0140-6736(03)12659-1.
[7] K.S. Park, et al., Functional characterization of two type III secretion systems of *Vibrio parahaemolyticus*, Infect. Immun. 72 (2004) 6659–6665, https://doi.org/10.1128/IAI.72.11.6659-6665.2004.
[8] T. Ono, et al., Identification of proteins secreted via *Vibrio parahaemolyticus* type III secretion system 1, Infect. Immun. 74 (2006) 1032–1042, https://doi.org/10.1128/IAI.74.2.1032-1042.2006.
[9] D.L. Burdette, J. Seemann, K. Orth, Vibrio VopQ induces PI3-kinase-independent autophagy and antagonizes phagocytosis, Mol. Microbiol. 73 (2009) 639–649, https://doi.org/10.1111/j.1365-2958.2009.06798.x.
[10] S. Matsuda, et al., A cytotoxic type III secretion effector of *Vibrio parahaemolyticus* targets vacuolar H^+-ATPase subunit c and ruptures host cell lysosomes, PLoS Pathog. 8 (2012) e1002803, https://doi.org/10.1371/journal.ppat.1002803.
[11] A. Sreelatha, et al., Vibrio effector protein, VopQ, forms a lysosomal gated channel that disrupts host ion homeostasis and autophagic flux, Proc. Natl. Acad. Sci. USA. 110 (2013) 11559–11564, https://doi.org/10.1073/pnas.1307032110.
[12] A. Sreelatha, et al., Vibrio effector protein VopQ inhibits fusion of V-ATPase-containing membranes, Proc. Natl. Acad. Sci. USA. 112 (2015) 100–105, https://doi.org/10.1073/pnas.1413764111.
[13] W. Peng, et al., A distinct inhibitory mechanism of the V-ATPase by Vibrio VopQ revealed by cryo-EM, Nat. Struct. Mol. Biol. 27 (2020) 589–597, https://doi.org/10.1038/s41594-020-0429-1.
[14] Y. Akeda, et al., Identification and characterization of a type III secretion-associated chaperone in the type III secretion system 1 of *Vibrio parahaemolyticus*, FEMS Microbiol. Lett. 296 (2009) 18–25, https://doi.org/10.1111/j.1574-6968.2009.01607.x.
[15] D. Liebschner, et al., Macromolecular structure determination using X-rays, neutrons and electrons: recent developments in Phenix, Acta Crystallogr. D Struct. Biol. 75 (2019) 861–877, https://doi.org/10.1107/S2059798319011471.
[16] P. Emsley, et al., Features and development of coot, Acta Crystallogr. D Biol. Crystallogr. 66 (2010) 486–501, https://doi.org/10.1107/S0907444910007493.
[17] C.J. Williams, et al., MolProbity: more and better reference data for improved all-atom structure validation, Protein Sci. 27 (2018) 293–315, https://doi.org/10.1002/pro.3330.
[18] T. Izoré, V. Job, A. Dessen, Biogenesis, regulation, and targeting of the type III secretion system, Structure 19 (2011) 603–612, https://doi.org/10.1016/j.str.2011.03.015.
[19] C. Parsot, C. Hamiaux, A.L. Page, The various and varying roles of specific chaperones in type III secretion systems, Curr. Opin. Microbiol. 6 (2003) 7–14, https://doi.org/10.1016/s1369-5274(02)00002-4.
[20] N.J. Vogelaar, et al., Analysis of the crystal structure of the ExsC.ExsE complex reveals distinctive binding interactions of the Pseudomonas aeruginosa type III secretion chaperone ExsC with ExsE and ExsD, Biochemistry 49 (2010) 5870–5879, https://doi.org/10.1021/bi100432e.
[21] S. Birtalan, P. Ghosh, Structure of the *Yersinia* type III secretory system chaperone SycE, Nat. Struct. Biol. 8 (2001) 974–978, https://doi.org/10.1038/nsb1101-974.
[22] Y. Luo, et al., Structural and biochemical characterization of the type III secretion chaperones CesT and SigE, Nat. Struct. Biol. 8 (2001) 1031–1036, https://doi.org/10.1038/nsb717.
[23] A. van Eerde, et al., Structure of Spa15, a type III secretion chaperone from Shigella flexneri with broad specificity, EMBO Rep. 5 (2004) 477–483, https://doi.org/10.1038/sj.embor.7400144.
[24] M. Lilic, M. Vujanac, C.E. Stebbins, A common structural motif in the binding of virulence factors to bacterial secretion chaperones, Mol. Cell 21 (2006) 653–664, https://doi.org/10.1016/j.molcel.2006.01.026.
[25] M. Vujanac, C.E. Stebbins, Context-dependent protein folding of a virulence peptide in the bacterial and host environments: structure of an SycH-YopH chaperone-effector complex, Acta Crystallogr. D Biol. Crystallogr. 69 (2013) 546–554, https://doi.org/10.1107/S0907444912051086.
[26] R. Janjusevic, et al., Structure of the HopA1(21-102)-ShcA chaperone-effector complex of *Pseudomonas syringae* reveals conservation of a virulence factor binding motif from animal to plant pathogens, J. Bacteriol. 195 (2013) 658–664, https://doi.org/10.1128/JB.01621-12.
[27] S. Dey, S. Datta, Interfacial residues of SpcS chaperone affects binding of effector toxin ExoT in *Pseudomonas aeruginosa*: novel insights from structural and computational studies, FEBS J. 281 (2014) 1267–1280, https://doi.org/10.1111/febs.12704.
[28] S.C. Birtalan, R.M. Phillips, P. Ghosh, Three-dimensional secretion signals in chaperone-effector complexes of bacterial pathogens, Mol. Cell 9 (2002) 971–980, https://doi.org/10.1016/s1097-2765(02)00529-4.
[29] F.D. Schubot, et al., Three-dimensional structure of a macromolecular assembly that regulates type III secretion in *Yersinia pestis*, J. Mol. Biol. 346 (2005) 1147–1161, https://doi.org/10.1016/j.jmb.2004.12.036.
[30] S. Miletic, et al., Substrate-engaged type III secretion system structures reveal gating mechanism for unfolded protein translocation, Nat. Commun. 12 (2021) 1546, https://doi.org/10.1038/s41467-021-21143-1.
[31] M.A. Larkin, et al., Clustal W and clustal X version 2.0, Bioinformatics 23 (2007) 2947–2948, https://doi.org/10.1093/bioinformatics/btm404.
[32] E.F. Pettersen, et al., UCSF Chimera—A visualization system for exploratory research and analysis, J. Comput. Chem. 25 (2004) 1605–1612, https://doi.org/10.1002/jcc.20084.
[33] D. Eisenberg, et al., Analysis of membrane and surface protein sequences with the hydrophobic moment plot, J. Mol. Biol. 179 (1984) 125–142, https://doi.org/10.1016/0022-2836(84)90309-7.
[34] A. Drozdetskiy, et al., JPred4: a protein secondary structure prediction server, Nucleic Acids Res. 43 (2015) W389–W394, https://doi.org/10.1093/nar/gkv332.